Communication of Bichromophore Emission upon Aggregation – Aroyl-*S,N*-ketene Acetals as Multifunctional Sensor Merocyanines

Lukas Biesen,[a] Lars May,[a] Nithiya Nirmalananthan-Budau,[b] Katrin Hoffmann,[b] Ute Resch-Genger,*[b] and Thomas J. J. Müller*[a]

Dedicated to Prof. Dr. Barry M. Trost on the occasion of his 80th birthday

Abstract: Aroyl-*S,N*-ketene acetal-based bichromophores can be readily synthesized in a consecutive three-component synthesis in good to excellent yields by condensation of aroyl chlorides and an *N*-(*p*-bromobenzyl) 2-methyl benzothiazolium salt followed by a Suzuki coupling, yielding a library of 31 bichromophoric fluorophores with substitution pattern-tunable emission properties. Varying both chromophores enables different communication pathways between the chromophores, exploiting aggregation-induced emission (AIE) and energy transfer (ET) properties, and thus, furnishing aggregation-based fluorescence switches. Possible applications range from fluorometric analysis of alcoholic beverages to pH sensors.

Introduction

Essential for the generation of novel functional organic dyes and molecular photonic materials is the control of involved communication pathways and intra- and intermolecular interactions.[1] This can be elegantly achieved with multichromophoric systems, consisting of covalently linked and spatially (within the range of the Förster radius) separated, nonconjugated fluorophores,[2] which interact by distance- and orientation-dependent energy transfer (ET) processes.[3] Switching from individually emitting fluorophores in solution to rigidized or aggregated systems in the solid-state, in aggregates or incorporated into nanoarchitectures can enable the tuning of the emission intensity and color, providing dual emission (aggregation induced dual emission, AIDE)[4] or white light generation for applications in photonic[5] and sensor technologies,[6] bioanalysis,[7] and medicinal diagnostics.[8] The increasingly popular concept behind such multichromophoric reporters and switches is aggregation induced emission (AIE)[9] or aggregation induced enhanced emission (AIEE).[10] These phenomena exploit deactivation of nonradiative pathways by restriction of intramolecular motions (RIM) or by restricted access to conical intersections (RACI).[10b] For fluorophore conjugates, which undergo partial or frustrated ET and also respond to external stimuli, such as solvent polarity, pH (e.g., by excited state intra-molecular proton transfer (ESIPT)),[11] or the presence of a specific target/analyte, multi-parametric responses can be generated.[12–14]

[a] *L. Biesen, Dr. L. May, Prof. Dr. T. J. J. Müller*
Institut für Organische Chemie und Makromolekulare Chemie
Heinrich-Heine-Universität Düsseldorf
Universitätsstraße 1, 40225 Düsseldorf (Germany)
E-mail: ThomasJJ.Mueller@hhu.de

[b] *Dr. N. Nirmalananthan-Budau, Dr. K. Hoffmann, Dr. U. Resch-Genger*
Division Biophotonics
Bundesanstalt für Materialforschung und -prüfung (BAM), Department 1
Richard-Willstätter-Straße 11, 12489 Berlin (Germany)
E-mail: ute.resch@bam.de

Supporting information for this article is available on the WWW under https://doi.org/10.1002/chem.202102052

Results and Discussion

Synthesis

Recently, we presented a novel AIE-active chromophore system with tunable solid-state emission utilizing aroyl-*S,N*-ketene acetals.[15] Essential for the occurrence of AIE is *N*-benzyl substitution. The promising photophysical and AIE properties of these chromophores encouraged us to develop a novel highly diversity-oriented, rapid modular one-pot synthesis[16] of *N*-benzyl aroyl *S,N*-ketene acetal bichromophores, implementing the *p*-bromo benzyl group for further functionalization and as coupling site for other nonconjugated chromophores. Optimization of a model reaction (see Supporting Information, chapter 3) with tetrakis(triphenylphosphane)palladium(0) as a catalyst and cesium carbonate as a base set the stage for concatenating a condensation-Suzuki coupling sequence in the sense of a consecutive three-component reaction in a one-pot fashion. Employing acid chlorides **1** bearing electron-donating or electron-withdrawing substituents or heterocyclic moieties (see

Supporting Information, Table S7), *N*-(*p*-bromobenzyl) 2-methyl benzothiazolium bromide (**2**)[15] and different boronic acid esters **3** comprising of blue-emitting core structures, such as triphenylamine, tri-phenylethene-dicarbazole, phenylcarbazole, perylene, and tetraphenyl-ethene,[17] a library of 31 aroyl-*S,N*-ketene acetal bichromophores **4** was synthesized in moderate to excellent yields of 31–96% (Figure 1).

The absorption and emission properties of the novel bichromophoric dyes **4** were studied in the solid state, in solvent mixtures of different polarity, and incorporated into polystyrene nanoparticles. In addition, two examples as potential sensor molecules were identified, utilizing dually emissive dyes for protonation studies and the determination of the water content of common alcoholic beverages.

Absorption and emission studies in the solid state

Previously, we showed that aroyl-*S,N*-ketene acetals account for a rainbow-type tuning of solid-state emission color[15] by variation of the electronic nature of the substituents in *para*-position of the aroyl moiety.[15,18] In a similar fashion, the bichromophores **4** can be readily distinguished by their solid-state emission color ranging from blue to orange-red depending both on the substituents in *para*-position of the aroyl moiety (R^1) and the second chromophore (R^2) (Figure 2). Phenylene carbazole bichromophore **4r** exhibits the shortest wavelength emission maximum (λ_{em} = 497 nm), while the *para*-cyanophenyl triarylamine bichromophore **4h** displays the most red-shifted emission maximum (λ_{em} = 600 nm) (Figure 2; for details see Supporting Information, chapter 7).

Solid-state fluorescence quantum yields (Φ_f) were determined for selected *para*-cyano substituted bichromophores.

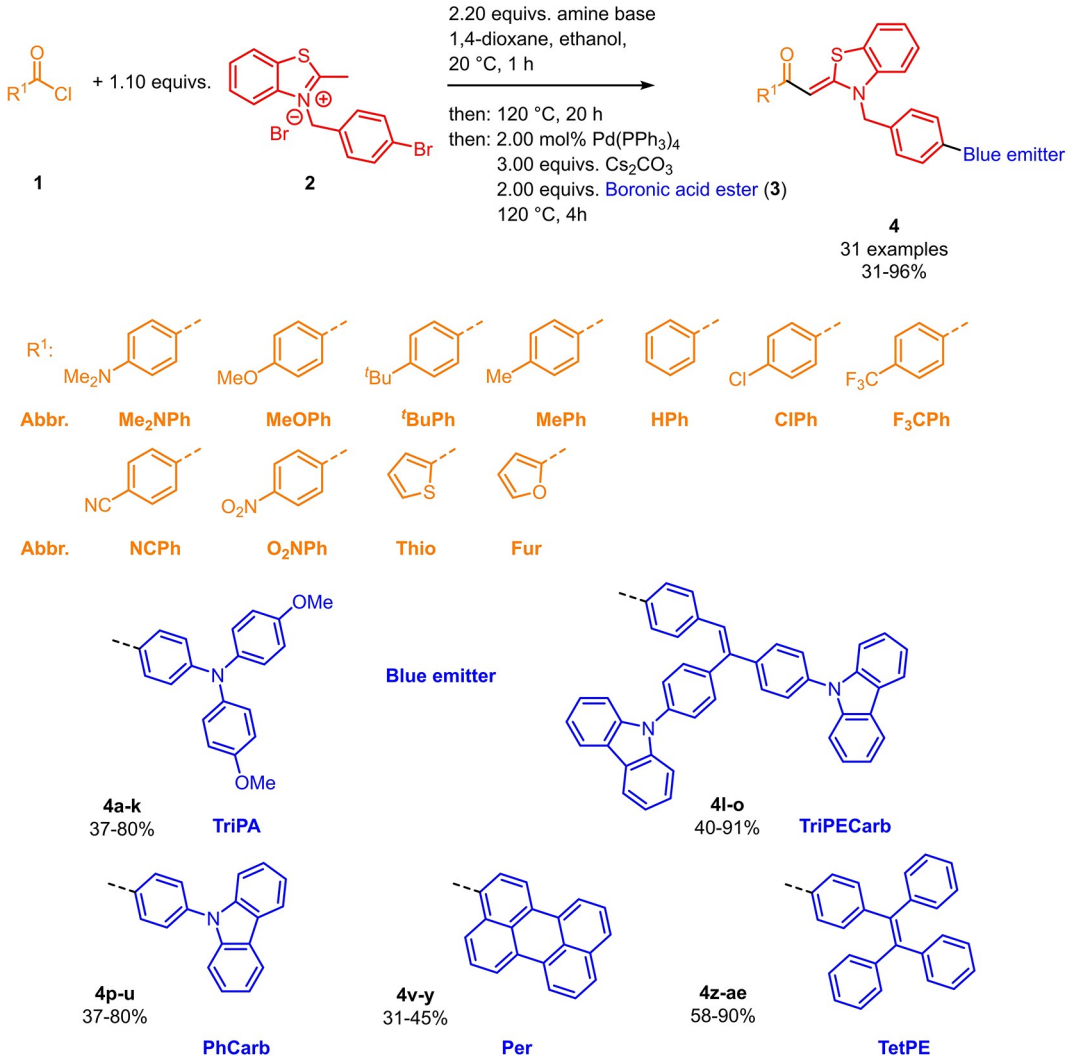

Figure 1. Consecutive three-component condensation-Suzuki coupling synthesis of aroyl-S,N-ketene acetal bichromophores 4 (all reactions were performed on a 0.50 mmol scale: **1** (0.50 mmol), **2** (0.55 mmol), amine base (1.1 mmol) in 1,4-dioxane/ethanol 3:1 (4.0 mL) were stirred at room temp for 1 h and at 120 °C for 20 h, then $Pd(PPh_3)_4$ (0.013 mmol), Cs_2CO_3 (1.50 mmol) and boronic acid ester **3** (1.0 mmol) were added and the reaction mixture stirred at 120 °C for 4 h; yields are given after flash chromatography on silica gel; for examples **4a**, **4l**, **4p**, **4v** and **4z**, diisopropylethylamine instead of triethylamine was used as an amine base and the ethanol was added in the Suzuki-coupling step).

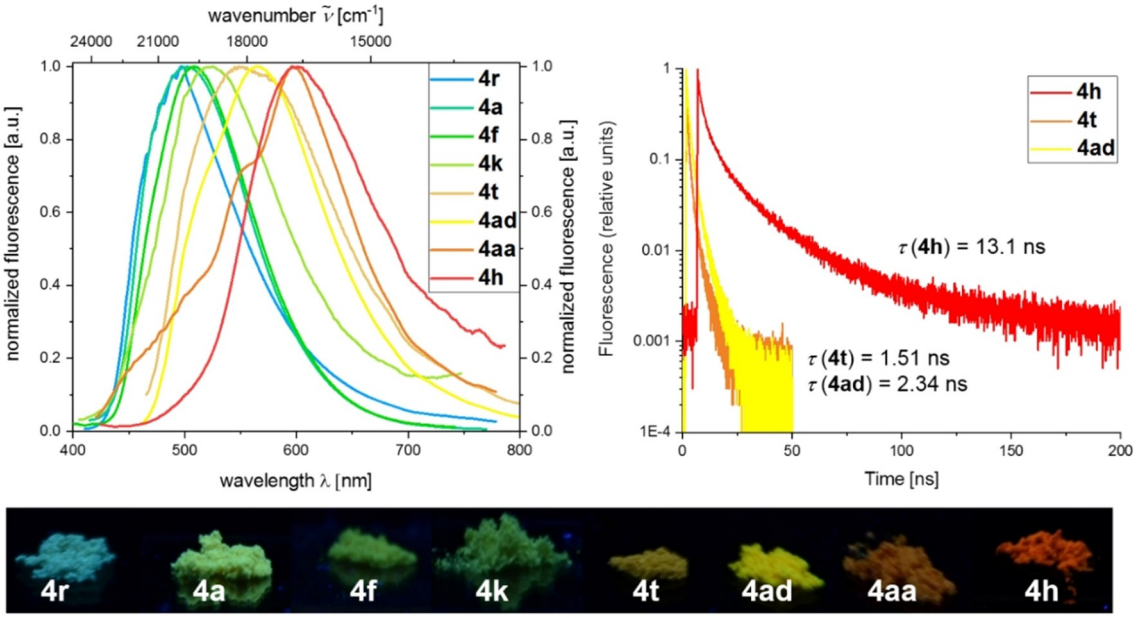

Figure 2. Top, left: normalized solid state emission spectra obtained with a calibrated fluorometer; top, right: fluorescence lifetimes of selected aroyl-*S,N*-ketene acetal bichromophores **4** ($\lambda_{exc} = \lambda_{abs,max}$ at $T = 298$ K); bottom: solid state fluorescence colors of selected aroyl-*S,N*-ketene acetal bichromophores **4** ($\lambda_{exc} = 365$ nm) revealing emission color tuning by substitution pattern.

While the triarylamine and phenylene carbazol bichromophores **4h** and **4t** exhibit only low Φ_f values of 0.01, the tetraphenylethene bichromophore **4ad** has an increased Φ_f of 0.06, presumably due to the solid-state emission of both chromophores.[9a,15] Three model bichromophores **4h**, **4t**, and **4ad** were selected as combinations of the red emissive *p*-cyano-phenyl-substituted aroyl-*S,N*-ketene acetal component and a blue luminescent chromophore, representing complementary emission partners. While compounds **4t** and **4ad** have lifetimes τ of 1.51 ($\lambda_{em} = 555$ nm) and 2.34 ns ($\lambda_{em} = 566$ nm) at $\lambda_{exc} = 330$ nm, *para*-cyanophenyl triarylamine bichromophore **4h** reveals a lifetime τ of 13.1 ns, which is astonishingly long for a red emitting fluorophore ($\lambda_{em} = 600$ nm) (Figure 2).[19] This long lifetime is tentatively ascribed to a complete ET from the triphenylamine to the aroyl-*S,N*-ketenacetal. This assumption is in line with the occurrence of a single emission maximum at $\lambda_{em} = 600$ nm upon excitation at 330 nm.

Absorption and fluorescence in ethanol

The absorption maxima of the series of aroyl-*S,N*-ketene acetal bichromophores **4** vary between 290 and 400 nm. While maxima around 400 nm can be ascribed to the aroyl-*S,N*-ketene acetal,[15] maxima covering a wavelength region from 290 to 330 nm can be unequivocally attributed to various blue emitters. Indeed, the bichromophores' absorption spectra match with the sum of the constituting chromophores.

The emission properties of the bichromophores **4** in solution are mostly governed by the blue emitters. In general, aroyl-*S,N*-ketene acetals do not intensely fluoresce in organic solvents.[15] The tetraphenylethene **4z–4ae** and triphenylethenyldicarbazole containing bichromophores **4l–4o** do not luminesce in any organic solvents but triphenylamine, phenylcarbazole, and perylene containing bichromophores **4p–4u** and **4v–4y** emit blue light in solution (for details, see Supporting Information, Table S5 and chapter 7). For selected examples **4h** and **4t**, Φ_f and τ in ethanol reach values between $\Phi_f = 0.03$ and 0.07 and $\tau = 2.13$ ns and 3.87 ns, respectively. Phenylcarbazole aroyl-*S,N*-ketene acetals **4p–4u** reveal a unique wavelength-depending solution photophysics upon excitation. Excitation at $\lambda_{exc} = 380$–400 nm leads to a weaker single emission maximum λ_{em} between 440 and 564 nm, comparable to the emission maxima of the corresponding aroyl-*S,N*-ketene acetal chromophores.[15] Excitation at 290 nm, thereby exciting the phenylcarbazol moiety ($\lambda_{em} = 380$ nm),[20] two emission maxima are observed arising from the emission of both chromophores. Consequently, a partial ET appears to be operative for PhCarb aroyl-*S,N*-ketene acetal bichromophores **4p–4u** (for details, see Supporting Information chapter 7).

Protonation in ethanol solutions

Triphenylamine and phenylene carbazol bichromophores further reveal a distinct halochromicity upon protonation with trifluoroacetic acid. In the absorption spectra, the spectral position of the longest wavelength maxima remains unchanged, but the intensity shifts hypochromically with increasing proton concentration (Figure 3, bottom left). However, a significant effect on the emission properties is induced upon protonation (Figure 3, bottom right). The fluorescence of

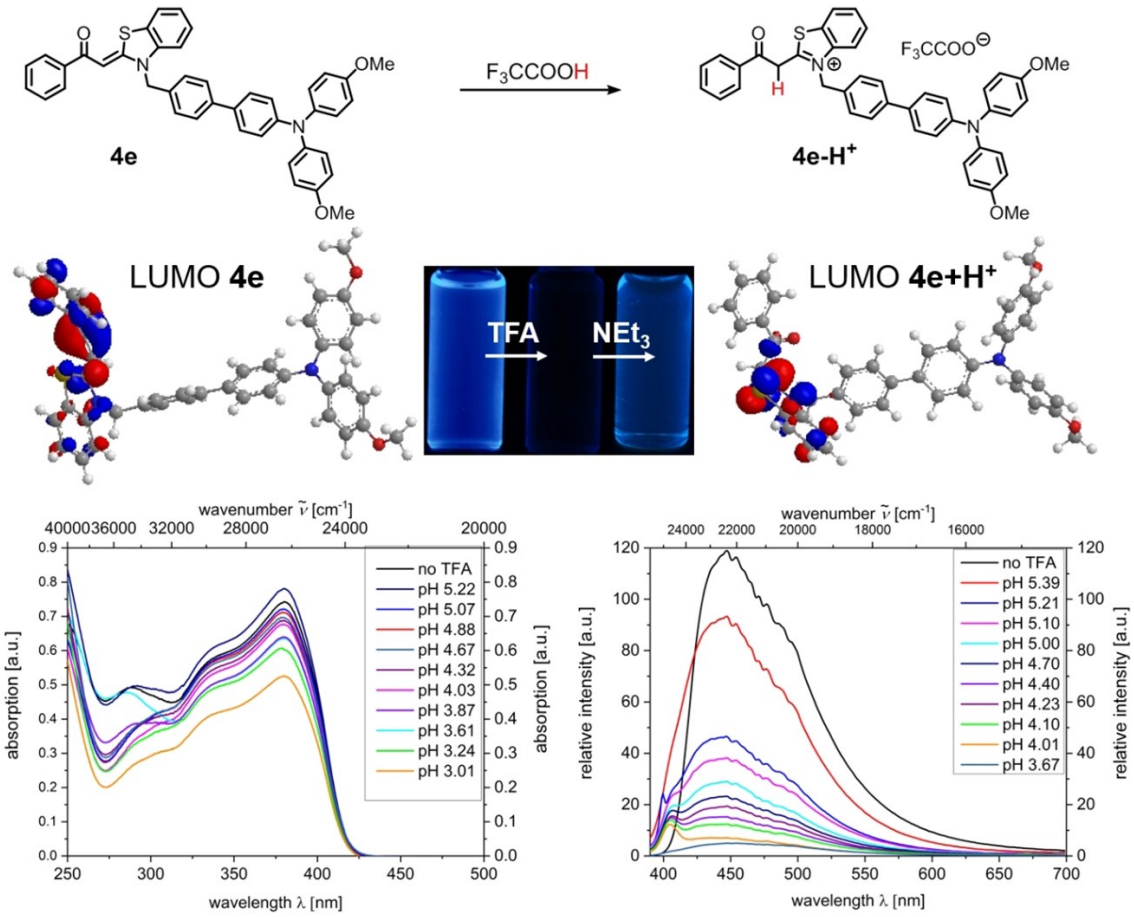

Figure 3. Top: Protonation of aroyl-*S,N*-ketene acetals using the example of **4e**; center, left and right: Kohn-Sham Molecular frontier orbitals of protonated bichromophore **4e**-H^+ using the polarizable continuum model (PCM) with ethanol (B3LYP/6-311G**, isosurface value at 0.04 a.u,); center, middle: Visual impression of **4e** in ethanol with addition of trifluoroacetic acid, followed by triethylamine upon excitation with a UV-lamp (λ_{exc} = 365 nm); bottom, left: Absorption spectra of **4e** in ethanol with increasing amount of trifluoroacetic acid (recorded at T = 298 K, c(**4e**) = 10^{-5} M); bottom, right: Emission spectra of **4e** in ethanol with increasing amount of trifluoroacetic acid (recorded at T = 298 K, c(**4e**) = 10^{-7} M, λ_{exc} = 404 nm).

protonated compound **4e** is quenched, however, upon adding triethylamine as a base the fluorescence is reinaugurated[21] (Figure 3, for details of measurements of **4r**, see Supporting Information, Figure S27). Therefore, this bichromophore may be used as a turn ON-OFF proton sensor by exploiting emission quenching upon protonation.

DFT calculations (B3LYP/6-311G**, applying PCM with ethanol as a solvent as implemented in Gaussian 09[22]) were performed to elucidate the protonation site of **4e**. For simplifying the calculation, we first performed calculations of the isolated aroyl-*S,N*-ketene acetal in the absence of the second chromophore. These model calculations reveal that the energetically most favored protonation site is the benzothiazole-α-methine carbon atom with $\Delta G = -3.98$ kcal/mol, compared to protonation at the aroyl oxygen atom (B3LYP/6-311G**, PCM ethanol; for details, see Supporting Information, chapter 8). These model calculations can be transferred to bichromophore **4e**, likewise assuming a similar first protonation at the methine carbon atom of the aroyl-*S,N*-ketene acetal.

This is in line with fluorescence quenching upon protonation due to a disruption of conjugation of the aroyl-*S,N*-ketene acetal π-system as indicated by the LUMO coefficient densities (Figure 3, center left). Moreover, the TD-DFT calculated absorption spectra of both **4e** and **4e**-H^+ very well reproduce the experimental data (for details, see Supporting Information, chapter 8). An NMR study of the protonated species further underlines the protonation of the pronounced methine carbon atom (see Supporting Information, chapter 6).

Aggregation induced emission (AIE) studies

All aroyl-*S,N*-ketene acetal chromophores show a characteristic AIE behavior, which in conjunction with the observed solid-state emission encouraged us to perform AIE studies with bichromophores **4**. Bichromophores **4** are soluble in common, polar organic solvents such as acetonitrile, THF, 1,4-dioxane, and ethanol, but insoluble in water. Hence, samples of the bichromophores were diluted in different organic solvent/water mixtures with water contents varying from 0 to 95%. As for aroyl-*S,N*-ketene acetals, the most distinct results were obtained in ethanol/water mixtures, which were subsequently used for all

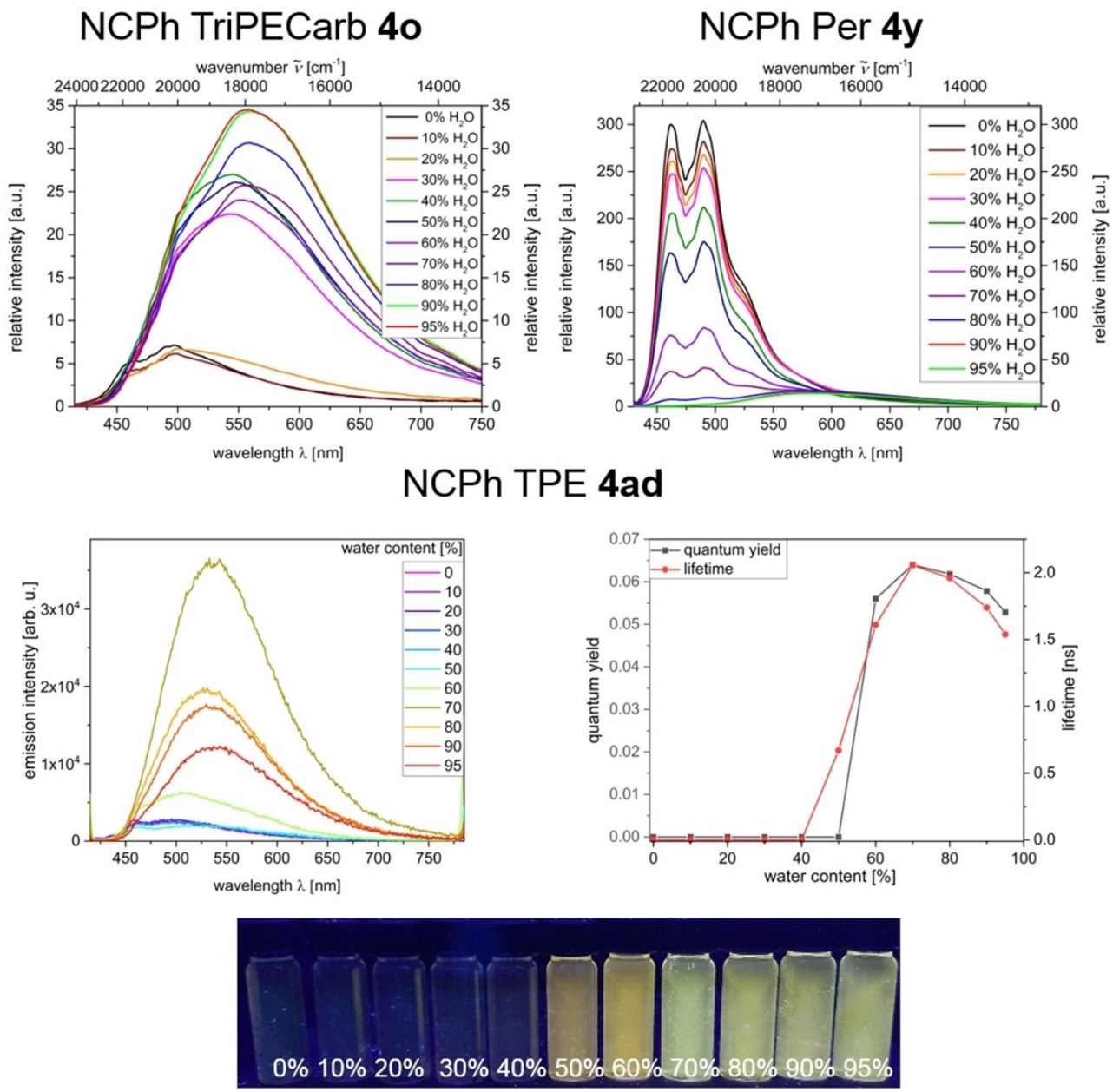

Figure 4. Top: Emission spectra of **4o** (left) and **4y** (right) in ethanol/water upon increasing water content (recorded at T = 298 K, c = 10^{-7} M, λ_{exc} (**4o**) = 400 nm, λ_{exc} (**4y**) = 442 nm; 2nd row: Emission spectra of **4ad** in ethanol/water upon increasing water content (recorded at T = 298 K, c = 10^{-7} M at λ_{exc} = 400 nm (left) and Φ_f and τ of **4ad** depending on the water fraction of the ethanol/water mixture (right); bottom: Visual impressions of the AIE features of **4ad** in ethanol/water mixtures of increasing water content upon excitation with a UV-lamp (λ_{exc} = 365 nm).

further AIE studies and will representatively be discussed in detail the *para*-cyano substituted examples of each class of bichromophores.

Triphenylethene dicarbazole and tetraphenylethene bichromophores **4o** and **4ad** show a similar emission behavior upon aggregation. At a low water fraction, the compounds fluoresce very weakly (Φ_f < 0.01). Upon increasing the water fraction, compounds **4o** and **4ad** start to aggregate, thus resulting in an enhanced Φ_f (0.07) and τ (2.06 ns).

Ascribing these effects to the blocking non-radiative decay of the excited singlet state by RIM or RACI is plausible.[9,10b] With a fluorescence increase by a factor of 20, the emission enhancement upon aggregation is most pronounced for bichromophore **4ad**.

Perylene aroyl-*S*,*N*-ketene acetal bichromophores **4v**–**4y** show aggregation-caused quenching (ACQ) behavior, which is typical for perylene chromophores[23] as exemplified by compound **4y**. At low water fractions, bichromophore **4y** fluoresces intensively blue. Increasing the water fraction, inducing aggregation, massively quenches the fluorescence. At a water fraction above 70%, the typical emission bands of perylene chromophores disappear indicating that the perylene subchromophore

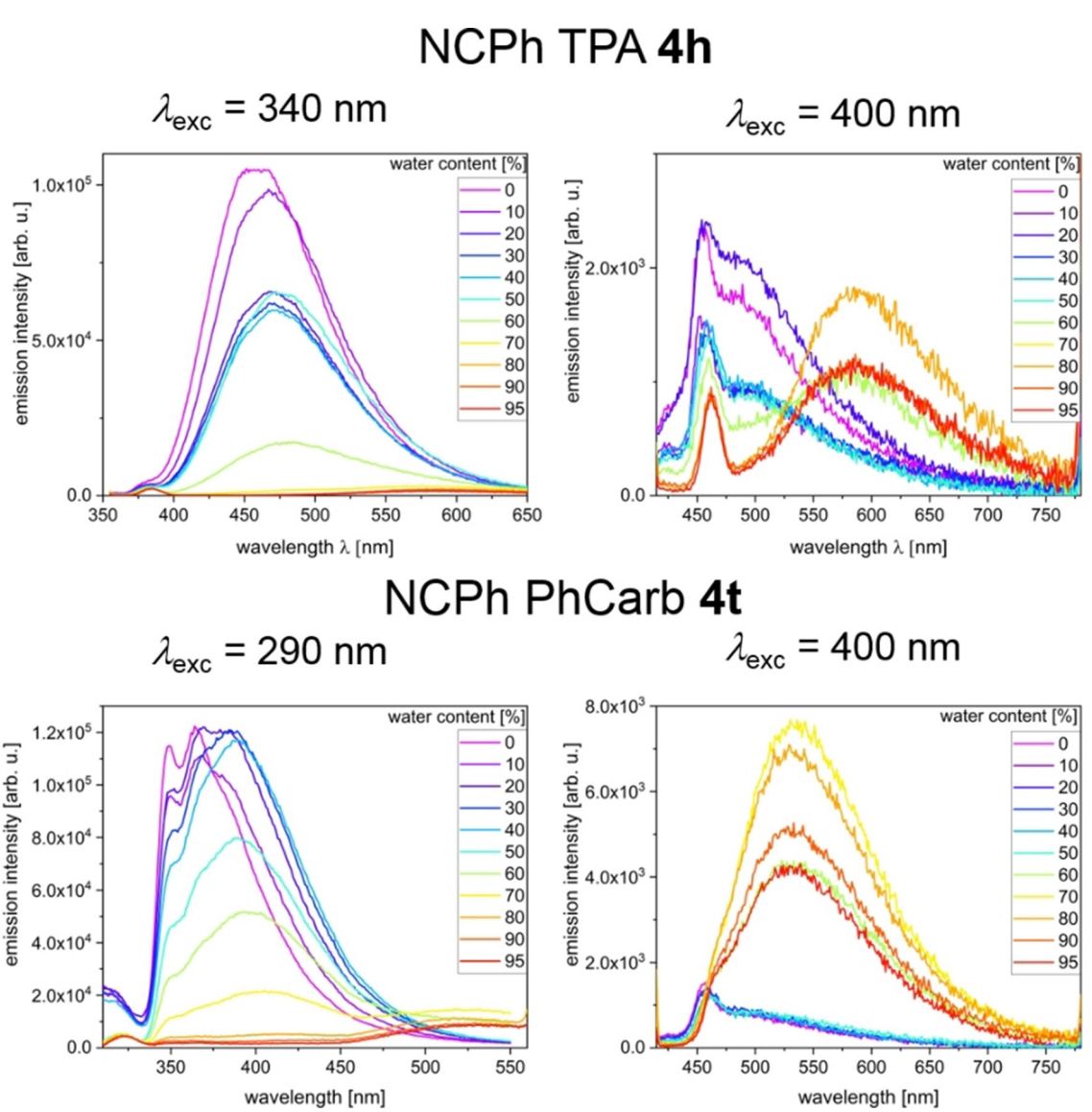

Figure 5. Emission spectra of **4h** in ethanol/water upon increasing water content (recorded at $T = 298$ K, $c = 10^{-7}$ M, λ_{exc} (**4h**) = 290 nm (left), λ_{exc} (**4h**) = 400 nm (right); bottom: Emission spectra of **4t** in ethanol/water upon increasing water content (recorded at $T = 298$ K, $c = 10^{-7}$ M, λ_{exc} (**4t**) = 290 nm (left), λ_{exc} (**4t**) = 400 nm (right).

is turned off, the emission bands are redshifted from 460 and 490 to 560 nm suggesting an excimer formation, simultaneously encompassing a loss of fluorescence intensity (Figure 4, top right) presenting perylene aroyl-*S,N*-ketene acetal bichromophores as aggregation off-switchable luminogens.

Investigating the AIE properties of triphenylamine and phenylene carbazole bichromophores reveals a different behavior paradigmatically shown by bichromophores **4h** and **4t**. Depending on the excitation wavelength λ_{exc}, the emission spectra differ. Upon exciting at 290 nm, the emission of the blue emitting chromophore can be harvested as well. For bichromophore **4h**, the emission band of the triphenylamine moiety at 477 nm ($\lambda_{exc} = 290$ nm) is completely quenched upon aggregation (see Supporting Information, Figure S49). Changing the blue emitting chromophore to phenylene carbazole, the phenylene carbazole emission band appears at 375 nm and is progressively attenuated upon further increase of the water content inducing aggregation. Φ_f and τ are both reduced upon aggregation (see Supporting Information, Figure S49). At a water fraction above 65% a second emission band occurs repetitively at 525 nm in each spectrum, which can be assigned to the aroyl-*S,N*-ketene acetal chromophore. This rare dual emission shows an equal intensity for both bands, thus, resulting in a mixed emission color suggesting an emerging ET (see Supporting Information, Figure S49). The dual fluorescence can be coined to the AIE characteristics of both chromophores in juxtaposition with solvent-induced changes of the spectral overlap of the emission of phenylenecarbazole acting as a donor and the aroyl-*S,N*-ketene acetal acting as an acceptor affecting the energy transfer efficiency. A partial (frustrated) energy transfer[4a,11a,24] from the phenylenecarbazole donor to

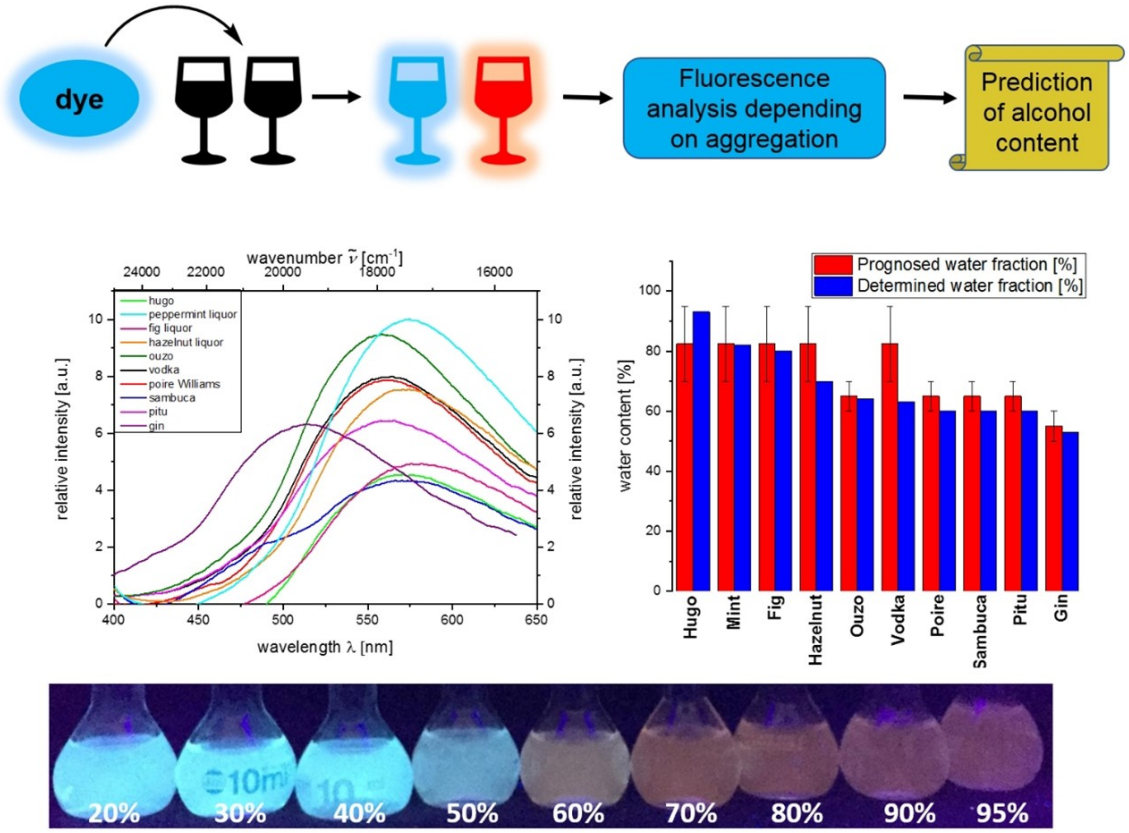

Figure 6. Top: Graphical illustration of alcohol content analysis; Middle, left: Emission spectra of **4 h** in different alcohols (recorded at $T = 298$ K, c(**4 h**) $= 10^{-7}$ M, $\lambda_{exc} = 400$ nm); Middle, right: Comparison between and determined water fraction; Bottom: Visual impression of **4 h** in ethanol/water mixtures with increasing water content ($\lambda_{exc} = 365$ nm).

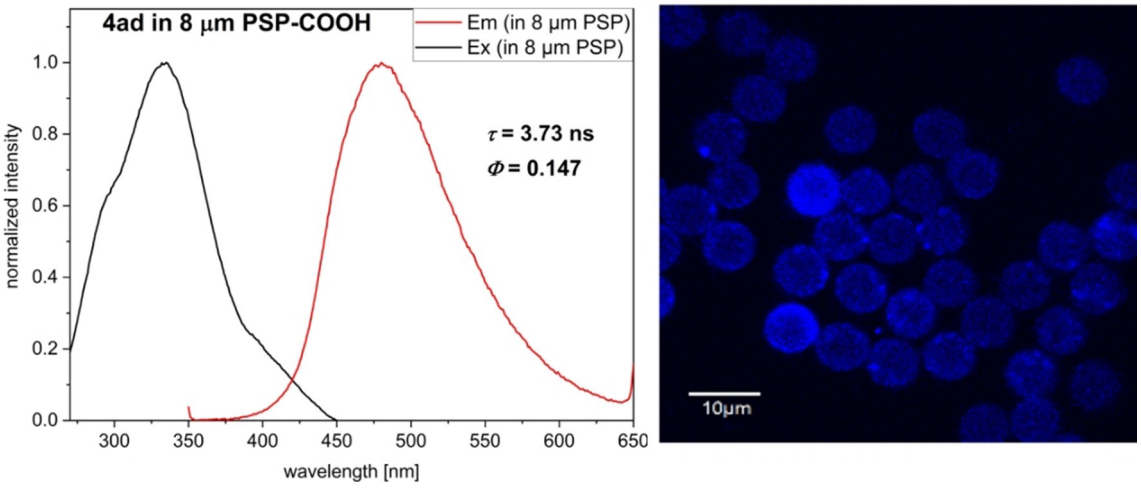

Figure 7. Normalized fluorescence excitation and emission spectra ($\lambda_{exc} = 401$ nm) of dispersed 8 µm-sized PSP loaded with dye **4 ad** (left) and CLSM image of the dye-loaded PSP (right).

the aroyl-*S*,*N*-ketene acetal acceptor may occur in the aggregate by both intra- and intermolecular energy transfer.

Upon selectively exciting the aroyl-*S*,*N*-ketene acetal part of the bichromophores at 400 nm a different behavior is obtained. For bichromophore **4 t**, a typical AIE behavior ascribed to the aroyl-*S*,*N*-ketene acetal moiety can be observed. At water fractions above 50%, the emission intensity increases by enforcing ongoing aggregation by raising the water fraction. The NCPh-TriPA bichromophore **4 h** fluoresces weakly, but upon aggregation τ is more than doubled from 3.50 to 8.11 ns

(Supporting Information Figure S49). At a water content of 20%, only the emission band of the triphenylamine was detected. A second pronounced maximum is detectable at 558–564 nm above a water content of 60%, giving rise to an aggregation-induced dual emission (AIDE) due to the contrasting AIE behavior of triphenylamine and aroyl-*S,N*-ketene acetal. This intertwining AIDE behavior can be exploited for polarity sensing (Figure 5, top right).[9a,25]

Determination of the water content of alcoholic beverages

Inspired by the emission color change upon aggregation (Figure 6, bottom), we tried to exploit this visual emission effect in solutions with different ethanol-water ratios for naked eye analytics. Anslyn[26] and Bunz[27] already used organic dyes for high-end discriminations of complex analytes, such as whiskey and other hard liquors by developing assays and chemical tongues. Here, we implement a rudimentary fluorescence-based tool for the naked-eye estimation of the water content of different alcoholic beverages. The NCPh–TriPA bichromophore **4h** was used for analyzing different colorless alcoholic beverages with a specified alcohol content. As shown in Figure 6, the emission spectra of **4h** in the different beverages vary in intensity and shape. By comparing the emission of **4h** in selected drinks to the results of previous AIE studies in ethanol-water mixtures (Figure 5 top), the water content of each drink could be visualized (Figure 6 top). Only Japanese rice wine, sake, could not be examined due to its native fluorescence. As summarized in Figure 6 and Table S8 (Supporting Information), only in case of the vodka sample, the optically determined water fraction overestimates the real water content.

Encapsulation of a bichromophore in polystyrene

Encapsulation of aroyl-*S,N*-ketene acetals in an nonpolar solid matrix like polystyrene led to a fluorescence enhancement due to steric restriction or attenuation of intramolecular rotations of the matrix-entrapped dye molecules.[15] To exemplify the influence of bead encapsulation on the emission of the bichromophores tetraphenylethene bichromophore **4ad** was chosen due to its intense solid-state fluorescence and pronounced AIE behavior. The results of encapsulating **4t** and **4ad** into 8 μm-sized carboxy-functionalized polystyrene particles (PSP) are detailed in the Supporting Information.[28] We chose a high encapsulation concentration of **4ad** (6 mM) to enhance the probability of dye-dye interactions in PSP. As confirmed by CLSM studies of single dye-stained particles the dye is homogeneously dispersed (Figure 7 right). The fluorescence excitation and emission spectra (Figure 7 left) of **4ad@PSP** reveal a hypsochromic shift of the respective maxima in comparison to the corresponding spectra in ethanol and ethanol-water mixtures, respectively, caused by the unpolar polystyrene matrix. Additionally, Φ_f is enhanced to 15% upon PSP encapsulation, exceeding Φ_f found for **4ad** in ethanol, ethanol-water mixtures, and in the solid state. Simultaneously, τ is increased to 3.73 ns.

Conclusion

In summary, a diverse library of emissive bichromophores was obtained with moderate to excellent yields by a concise consecutive three-component condensation-Suzuki synthesis of *N*-benzyl aroyl *S,N*-ketene acetal bichromophores in a one-pot fashion. Spectroscopic studies of these differently substituted bichromophores in the solid state, in organic solvents, upon aggregation, and upon encapsulation into polystyrene particles reveal substitution pattern control of the solid-state emission color and the aggregation-induced emission (AIE). Variation of the blue emitting chromophore allows elaboration of different communication pathways between the ligated chromophores, such as complete or partial energy transfer leading to a dual emission or an aggregation-induced switching of the fluorescence. The AIE chromicity of the dyes is well suited for analyte screening and sensing as demonstrated by the analysis of the water content of alcoholic beverages based on the extent of the AIE color shifts. Our results underline that the rational design of novel bichromophoric systems for multifunctional chromophore applications requires a detailed understanding of (partial) energy transfer in aggregates. This work is currently addressed by tailored sets of aroyl-*S,N*-ketene acetals.

Acknowledgements

The authors cordially thank the Fonds der Chemischen Industrie and the Deutsche Forschungsgemeinschaft (Mu 1088/9-1) for financial support. Open access funding enabled and organized by Projekt DEAL.

Conflict of Interest

The authors declare no conflict of interest.

Keywords: aggregation-induced emission · aroyl-*S,N*-ketene acetals · bichromophores · energy transfer · fluorescence · one-pot synthesis

[1] a) G. C. Bazan, *J. Org. Chem.* **2007**, *72*, 8615–8635; b) Z. Yoshida, T. Kitao, *International Symposium in Osaka as the 70th Anniversary of the Founding Proceeding*, Kinki Chemical Society, Mita Press, Tokyo **1989**.

[2] a) A. Lapini, P. Fabbrizzi, M. Piccardo, M. di Donato, L. Lascialfari, P. Foggi, S. Cicchi, M. Biczysko, I. Carnimeo, F. Santoro, *Phys. Chem. Chem. Phys.* **2014**, *16*, 10059–10074; b) A. S. Klymchenko, V. G. Pivovarenko, T. Ozturk, A. P. Demchenko, *New J. Chem.* **2003**, *27*, 1336–1343; c) A. S. Klymchenko, D. A. Yushchenko, Y. Mély, *J. Photochem. Photobiol. A* **2007**, *192*, 93–97.

[3] a) Q. Y. Yang, J. M. Lehn, *Angew. Chem.* **2014**, *126*, 4660–4665; *Angew. Chem. Int. Ed.* **2014**, *53*, 4572–4577; b) Z. Zhang, Y.-S. Wu, K.-C. Tang, C.-L. Chen, J.-W. Ho, J. Su, H. Tian, P.-T. Chou, *J. Am. Chem. Soc.* **2015**, *137*, 8509–8520; c) B. Xu, Y. Mu, Z. Mao, Z. Xie, H. Wu, Y. Zhang, C. Jin, Z. Chi, S. Liu, J. Xu, *Chem. Sci.* **2016**, *7*, 2201–2206.

[4] a) M. Denißen, R. Hannen, D. Itskalov, L. Biesen, N. Nirmalananthan-Budau, K. Hoffmann, G. J. Reiss, U. Resch-Genger, T. J. J. Müller, *Chem. Commun.* **2020**, *56*, 7407–7410; b) Z. He, W. Zhao, J. W. Lam, Q. Peng, H. Ma, G. Liang, Z. Shuai, B. Z. Tang, *Nat. Commun.* **2017**, *8*, 1–8; c) C. Yuan, S. Saito, C. Camacho, S. Irle, I. Hisaki, S. Yamaguchi, *J. Am. Chem. Soc.* **2013**, *135*, 8842–8845.

[5] a) M. Börgardts, T. J. J. Müller, *Beilstein J. Org. Chem.* **2017**, *13*, 768–778; b) L. Xie, Y. Chen, W. Wu, H. Guo, J. Zhao, X. Yu, *Dyes Pigm.* **2012**, *92*, 1361–1369; c) M. Tominaga, H. Naito, Y. Morisaki, Y. Chujo, *New J. Chem.* **2014**, *38*, 5686–5690; d) M. D. Bilokin, V. V. Shvadchak, D. A. Yushchenko, A. S. Klymchenko, G. Duportail, Y. Mely, V. G. Pivovarenko, *Tetrahedron Lett.* **2009**, *50*, 4714–4719.

[6] a) A. Ajayaghosh, E. Arunkumar, J. Daub, *Angew. Chem.* **2002**, *114*, 1844–1847; *Angew. Chem. Int. Ed.* **2002**, *41*, 1766–1769; b) M. Vera, H. Santacruz Ortega, M. Inoue, L. Machi, *Supramol. Chem.* **2019**, *31*, 336–348; c) N. I. Georgiev, A. I. Said, R. A. Toshkova, R. D. Tzoneva, V. B. Bojinov, *Dyes Pigm.* **2019**, *160*, 28–36; d) X. Li, G. Baryshnikov, C. Deng, X. Bao, B. Wu, Y. Zhou, H. Ågren, L. Zhu, *Nat. Commun.* **2019**, *10*, 1–9.

[7] A. S. Klymchenko, *Acc. Chem. Res.* **2017**, *50*, 366–375.

[8] G. Zhang, G. M. Palmer, M. W. Dewhirst, C. L. Fraser, *Nat. Mater.* **2009**, *8*, 747–751.

[9] a) J. Mei, N. L. Leung, R. T. Kwok, J. W. Lam, B. Z. Tang, *Chem. Rev.* **2015**, *115*, 11718–11940; b) J. Mei, Y. Hong, J. W. Lam, A. Qin, Y. Tang, B. Z. Tang, *Adv. Mater.* **2014**, *26*, 5429–5479.

[10] a) B.-K. An, S.-K. Kwon, S.-D. Jung, S. Y. Park, *J. Am. Chem. Soc.* **2002**, *124*, 14410–14415; b) F. Würthner, *Angew. Chem.* **2020**, *59*, 14296–14301; *Angew. Chem. Int. Ed.* **2020**, *59*, 14192–14196.

[11] a) S. Park, J. E. Kwon, S. H. Kim, J. Seo, K. Chung, S.-Y. Park, D.-J. Jang, B. M. Medina, J. Gierschner, S. Y. Park, *J. Am. Chem. Soc.* **2009**, *131*, 14043–14049; b) J. E. Kwon, S. Park, S. Y. Park, *J. Am. Chem. Soc.* **2013**, *135*, 11239–11246; c) K. Benelhadj, W. Muzuzu, J. Massue, P. Retailleau, A. Charaf-Eddin, A. D. Laurent, D. Jacquemin, G. Ulrich, R. Ziessel, *Chem. Eur. J.* **2014**, *20*, 12843–12857.

[12] a) J. Tydlitát, S. Achelle, J. Rodríguez-López, O. Pytela, T. Mikýsek, N. Cabon, F. Robin-le Guen, D. Miklík, Z. Růžičková, F. Bureš, *Dyes Pigm.* **2017**, *146*, 467–478; b) E. Täuscher, D. Weiß, R. Beckert, J. Fabian, A. Assumpção, H. Görls, *Tetrahedron Lett.* **2011**, *52*, 2292–2294.

[13] a) B. Xu, Z. Chi, X. Zhang, H. Li, C. Chen, S. Liu, Y. Zhang, J. Xu, *Chem. Commun.* **2011**, *47*, 11080–11082; b) C. Li, W.-L. Gong, Z. Hu, M. P. Aldred, G.-F. Zhang, T. Chen, Z.-L. Huang, M.-Q. Zhu, *RSC Adv.* **2013**, *3*, 8967–8972.

[14] a) Z. Chang, Y. Jiang, B. He, J. Chen, Z. Yang, P. Lu, H. S. Kwok, Z. Zhao, H. Qiu, B. Z. Tang, *Chem. Commun.* **2013**, *49*, 594–596; b) Z. Zhao, C. Y. Chan, S. Chen, C. Deng, J. W. Lam, C. K. Jim, Y. Hong, P. Lu, Z. Chang, X. Chen, *J. Mater. Chem.* **2012**, *22*, 4527–4534; c) X. Cai, D. Mao, C. Wang, D. Kong, X. Cheng, B. Liu, *Angew. Chem.* **2018**, *130*, 16634–16638; *Angew. Chem. Int. Ed.* **2018**, *57*, 16396–16400; d) X. Cai, B. Liu, *Angew. Chem.* **2020**, *132*, 9952–9970; *Angew. Chem. Int. Ed.* **2020**, *59*, 9868–9886; e) J. W. Hong, H. Benmansour, G. C. Bazan, *Chem. Eur. J.* **2003**, *9*, 3186–3192.

[15] L. Biesen, N. Nirmalananthan-Budau, K. Hoffmann, U. Resch-Genger, T. J. J. Müller, *Angew. Chem.* **2020**, *132*, 10123–10127; *Angew. Chem. Int. Ed.* **2020**, *59*, 10037–10041.

[16] For recent reviews on multicomponent syntheses of functional chromophores and luminophores, see for example a) L. Levi, T. J. J. Müller, *Chem. Soc. Rev.* **2016**, *45*, 2825–2846; b) L. Levi, T. J. J. Müller, *Eur. J. Org. Chem.* **2016**, 2907–2918; c) F. K. Merkt, T. J. J. Müller, *Isr. J. Chem.* **2018**, *58*, 889–900; d) T. J. J. Müller, *Drug Discovery Today Technol.* **2018**, *29*, 19–26.

[17] a) R. Rybakiewicz, M. Zagorska, A. Pron, *Chem. Pap.* **2017**, *71*, 243–268; b) Z. Yang, Z. Chi, Z. Mao, Y. Zhang, S. Liu, J. Zhao, M. P. Aldred, Z. Chi, *Mater. Chem. Front.* **2018**, *2*, 861–890; c) G. Sathiyan, E. Sivakumar, R. Ganesamoorthy, R. Thangamuthu, P. Sakthivel, *Tetrahedron Lett.* **2016**, *57*, 243–252.

[18] a) M. Shimizu, Y. Takeda, M. Higashi, T. Hiyama, *Angew. Chem.* **2009**, *121*, 3707–3710; *Angew. Chem. Int. Ed.* **2009**, *48*, 3653–3656; b) A. Wakamiya, K. Mori, S. Yamaguchi, *Angew. Chem.* **2007**, *119*, 4351–4354; *Angew. Chem. Int. Ed.* **2007**, *46*, 4273–4276.

[19] a) U. Resch-Genger, M. Grabolle, S. Cavaliere-Jaricot, R. Nitschke, T. Nann, *Nat. Methods* **2008**, *5*, 763–775; b) M. Y. Berezin, S. Achilefu, *Chem. Rev.* **2010**, *110*, 2641–2684.

[20] J. Yuan, L. Jin, R. Chen, X. Tang, X. Xie, Y. Tang, W. Huang, *New J. Chem.* **2018**, *42*, 14704–14708.

[21] O. Stern, M. Volmer, *Phys. Z.* **1919**, *20*, 183–188.

[22] M. J. Frisch, G. W. Trucks, H. B. Schlegel, G. E. Scuseria, M. A. Robb, J. R. Cheeseman, G. Scalmani, V. Barone, B. Mennucci, G. A. Petersson, H. Nakatsuji, M. Caricato, X. Li, H. P. Hratchian, A. F. Izmaylov, J. Bloino, G. Zheng, J. L. Sonnenberg, M. Hada, M. Ehara, K. Toyota, R. Fukuda, J. Hasegawa, M. Ishida, T. Nakajima, Y. Honda, O. Kitao, H. Nakai, T. Vreven, J. A. Montgomery Jr., J. E. Peralta, F. Ogliaro, M. Bearpark, J. J. Heyd, E. Brothers, K. N. Kudin, V. N. Staroverov, R. Kobayashi, J. Normand, K. Raghavachari, A. Rendell, J. C. Burant, S. S. Iyengar, J. Tomasi, M. Cossi, N. Rega, J. M. Millam, M. Klene, J. E. Knox, J. B. Cross, V. Bakken, C. Adamo, J. Jaramillo, R. Gomperts, R. E. Stratmann, O. Yazyev, A. J. Austin, R. Cammi, C. Pomelli, J. W. Ochterski, R. L. Martin, K. Morokuma, V. G. Zakrzewski, G. A. Voth, P. Salvador, J. J. Dannenberg, S. Dapprich, A. D. Daniels, O. Farkas, J. B. Foresman, J. V. Ortiz, J. Cioslowski, D. J. Fox, *Gaussian 09, Revision A.02* **2009**.

[23] W. Z. Yuan, P. Lu, S. Chen, J. W. Lam, Z. Wang, Y. Liu, H. S. Kwok, Y. Ma, B. Z. Tang, *Adv. Mater.* **2010**, *22*, 2159–2163.

[24] Y. Lei, Q. Liao, H. Fu, J. Yao, *J. Am. Chem. Soc.* **2010**, *132*, 1742–1743.

[25] S. Mukherjee, P. Thilagar, *Chem. Eur. J.* **2014**, *20*, 9052–9062.

[26] S. L. Wiskur, E. V. Anslyn, *J. Am. Chem. Soc.* **2001**, *123*, 10109–10110.

[27] a) J. Han, M. Bender, K. Seehafer, U. H. F. Bunz, *Angew. Chem.* **2016**, *128*, 7820–7823; *Angew. Chem. Int. Ed.* **2016**, *55*, 7689–7692; b) J. Han, C. Ma, B. Wang, M. Bender, M. Bojanowski, M. Hergert, K. Seehafer, A. Herrmann, U. H. F. Bunz, *Chem* **2017**, *2*, 817–824; c) B. Wang, J. Han, H. Zhang, M. Bender, A. Biella, K. Seehafer, U. H. Bunz, *Chem. Eur. J.* **2018**, *24*, 17361–17366.

[28] a) T. Behnke, C. Würth, K. Hoffmann, M. Hübner, U. Panne, U. Resch-Genger, *J. Fluoresc.* **2011**, *21*, 937–944; b) T. Behnke, C. Würth, E.-M. Laux, K. Hoffmann, U. Resch-Genger, *Dyes Pigm.* **2012**, *94*, 247–257.

Manuscript received: June 10, 2021
Accepted manuscript online: June 25, 2021
Version of record online: August 1, 2021

